

Supporting Information

Extracellular Electron Transfer Across Bio-Nano Interfaces for CO₂ Electroreduction

Zhaodong Li[†], Wei Xiong[‡], Bertrand J. Tremolet de Villers[†], Chao Wu[‡], Ji Hao[†], Drazenka Svedruzic^{**}, Jeffrey L. Blackburn^{**}

[‡]Biosciences Center and [†]Chemistry and Nanoscience Center, National Renewable Energy Laboratory, 1617 Cole Boulevard, Golden, Colorado 80401, United States

**Corresponding authors: Drazenka Svedruzic, Jeffrey L. Blackburn*

METHODS

Preparation of single wall carbon nanotube (SWCNT) dispersions

Plasma-torch (PT) semiconducting single wall carbon nanotubes (s-SWCNTs) powders were purchased from NanoIntegris (Quebec, Canada). Inks containing dispersed SWCNTs were prepared based on a previous report.¹ Briefly, a removable ‘supra-molecular’ polymer (SMP), synthesized in-house, was mixed with toluene (2 mg ml⁻¹), and then stirred at 78 °C till the polymer was well dissolved. The SMP polymer utilized here was first reported by Zhenan Bao’s group²: 1,1’-(((1*E*,1’*E*)-(9,9-didodecyl-9*H*-fluorene-2,7-diyl)bis(ethene-2,1-diyl))bis(6-methyl-4-oxo-1,4-dihydropyrimidine-5,2-diyl))bis(3-dodecylurea). Thereafter, SWCNT powders (7.5 mg) were added into the pre-prepared polymer-toluene solution (0.5 mg ml⁻¹). This blend was sonicated by tip-sonicator (Cole-Palmer CPX 750) with 40% of amplitude for 15 min in a water bath. The black slurry was transferred to the thin-wall centrifuge tube and centrifuged for 5 minutes in SW 32 Ti rotor at 13,200 rpm, 20 °C in a Beckman Coulter L-100 XP ultracentrifuge to generate a compacted pellet and supernatant rich in PT-SWCNTs. The top supernatant was carefully collected and transferred to the thick-wall centrifuge tube for an additional centrifugation step (24,100 rpm, 20 hours, 20 °C). The supernatant was removed and the PT-SWCNTs pellets were gently rinsed with toluene before being re-dispersed in neat toluene solution using gentle bath sonication. The sonication and the polymer-exchange step were repeated 2 times. To monitor that the excess SMP polymer removal, UV-vis-NIR spectra were collected (Fig. S1a). As prepared PT-SWCNT ink was used in the next step to functionalize carbon felt (CF).

Preparation of CF and SWCNT functionalized CF electrodes (CF/SWCNT)

Carbon felt (AvCrab Felt G100, Fuel Cell Store) as received was cut into pieces with the rectangular shape of 2 × 1 cm, and thickness 0.3 cm. For SWCNT-functionalization CF pieces were soaked for 2 h in the prepared SWCNT ink. Next, the samples were immersed into hot toluene (78 °C) and trifluoroacetic (TFA)/toluene (10 µl/ml) for 5 min and 2 min, respectively. As discussed in detail in our previous study¹, the TFA treatment is used to completely remove the dispersing polymer, which in this study ensures that we form an intimate interface between the SWCNTs and *C. lj.* bacteria. Next, CF/SWCNT samples were subjected to toluene rinse cycles where each cycle consists of (1) soaking in hot toluene for an additional 1 hour and then (2) washing in toluene for 5 min at room temperature. Finally, CF/SWCNT samples were dried in vacuum overnight before

the utilization. In order to produce the CF/SWCNT electrodes functionalized with different amount of SWCNTs, SWCNT ink, prepared as described above (C_0), was diluted to various concentrations (C/C_0) 0.01, 0.10, 0.25, 0.75 and 1 which were then used to prepare CF/SWCNT electrodes (Fig S1c). These electrodes were analyzed by Raman mapping to confirm and visualize the increased SWCNT coverage on C-felt when prepared with higher concentrations inks (Fig S1b,d). Scanning 2D Raman microscope images were collected using a Renishaw inVia confocal Raman microscope. Images were acquired with a 100 × magnification objective. The excitation was 532nm an Nd:YAG laser with a doubling crystal. Laser power was set to 5% of total power (5% total power ~ 0.5 mW). Each pixel was an average of 5 accumulations at 1 second exposure per accumulation.

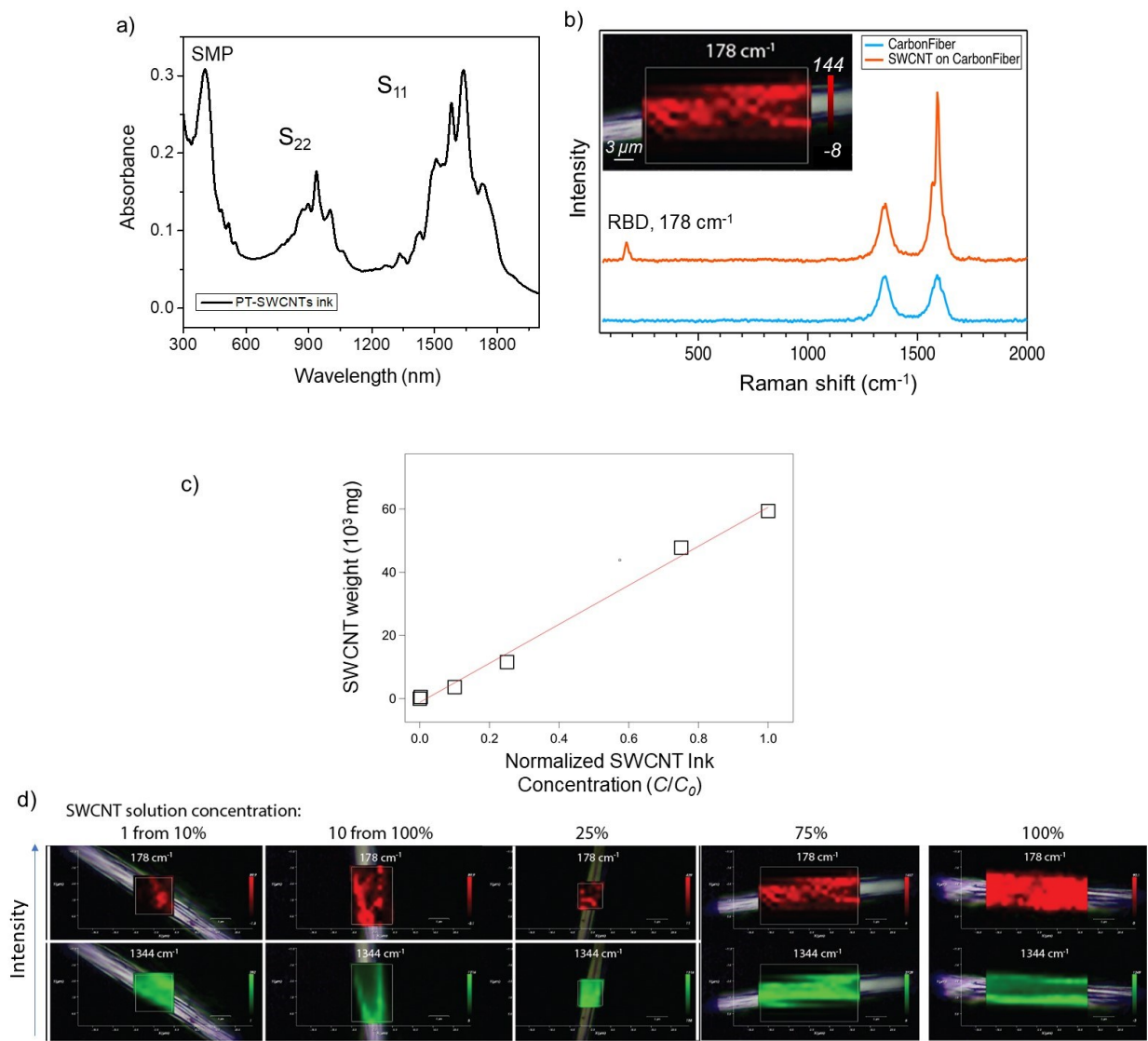


Figure S1. a) UV-vis-NIR spectra of as-prepared SWCNT ink used for CF functionalization. **b)** Raman spectra and Raman imaging of SWCNT-functionalized C-fiber. The Radial Breathing Mode (RBM) modes at 178 cm^{-1} as well as the sharp “G band” peak at 1590 cm^{-1} are characteristic for SWCNT film. The spectra were collected by focusing on either C-fiber section of surface uncovered and covered with SWCNT films. Inset shows an optical microscope image of a SWCNT-coated C-felt fiber (gray), on top of which is superimposed the Raman intensity map of the SWCNT RBM at 178 cm^{-1} (red) for a selected fiber area. **c)** SWCNT quantities for each electrode were estimated based on differences in UV-vis-NIR spectra of the SWCNT ink before and after C-felt soak. **d)** Raman mapping to confirm and visualize the SWCNT coverage on C-felt when prepared with different concentrations inks. Gray - optical image of a carbon fiber; Red -

spatial map recorded at 178 cm^{-1} , which is characteristic signal for SWCNTs radial breathing mode; Green - spatial map of signal recorder at 1344 cm^{-1} , which is graphitic carbon signal.

Characterization of CF and CF/SWCNT electrodes

SEM images of carbon fiber and SWCNT-functionalized carbon fiber are shown below (Fig. S2a,b).

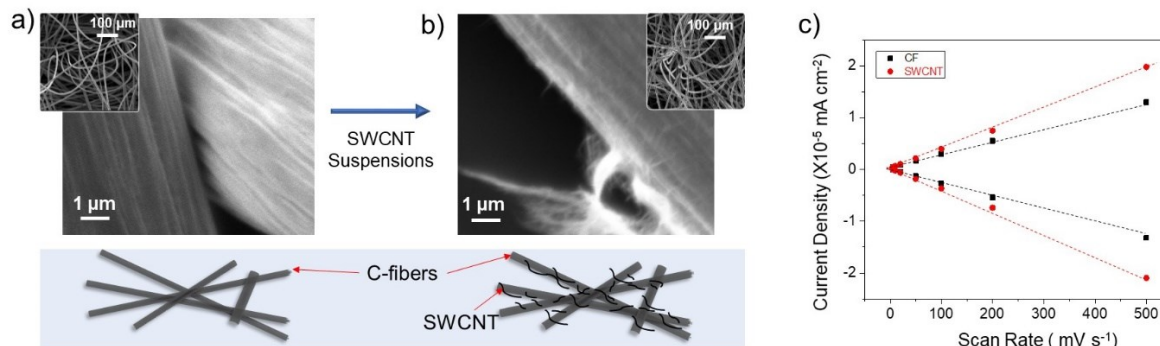


Figure S2. a) Scanning electron microscopy (SEM) images of carbon felt fiber. b) After soaking of C-felt in the s-SWCNT suspension, the SWCNT films appears as “hair-like” features on the carbon fiber surface. b) Capacitance measurements conducted in PETC media (-trace metals, -vitamins); were collected at 0 V vs Ag/AgCl (i.e. non-faradic currents).

We measured capacitance for CF and CF/SWCNT electrodes to determine the difference in electroactive surfaces due to the SWCNT-functionalization. Figure S2b show representative set of data for plain CF and CF/SWCNT films. By comparing slopes in the graph we can calculate the increases in electroactive surface of CF after SWCNT functionalization.

Clostridium ljungdahlii cultures

C. ljungdahlii DSM 13528 (ATCC 55383) was purchased from the *German Collection of Microorganisms and Cell Cultures* (DSMZ) and maintained by freezing mid-log-phase cultures at $-80\text{ }^{\circ}\text{C}$ with 10% dimethyl sulfoxide (DMSO) for long-term storage. An inoculum of *Clostridium ljungdahlii* (10% (v/v) *C. ljungdahlii* DMSO stock) was grown under strict anaerobic conditions in 20 ml modified YTF (**Y**east extract-**T**ripton-**F**ructose) media in a batch tube at $37\text{ }^{\circ}\text{C}$. Usually, the OD 600 nm of the inoculum was ~ 2.0 after 3-day growth.

YTF medium:

10 gL⁻¹ fructose

10 gL⁻¹ yeast extract

16 gL⁻¹ tryptone

4 gL⁻¹ sodium chloride

Growth of *C. ljungdahlii* biofilms on CF and CF/SWCNT electrodes (*Growth phase*):

For electro-bioreactor we used typical H-cells with three-electrode configuration (Fig. S3). The volume of the cell was 150 ml and both catholyte and anolyte volume were 65 ml. Electrolyte was stirred by bubbling CO₂/N₂ gas. As a reference electrode we used aqueous Ag/AgCl (saturated) (CH Instruments, Inc). The counter electrode was flat Pt foil with dimensions of 1x1 cm². Composition of electrolyte in both anode and cathode compartment was the same at the beginning of each experiment. A Nafion 117 membrane (Sigma-Aldrich) was used to separate the cathodic from anodic compartment. The purging gas (CO₂ : N₂ = 20%:80%) for each chamber could be independently controlled with typical flow rate of 5 sccm. For biofilm growth we used either CF or CF/SWCNT electrode, with applied reducing potential. CF without applied reducing potential was also conducted for control experiment. When constant reducing potential was applied (-0.7 V vs. Ag/AgCl), amperometric (i-t) measurements were conducted to monitor electron consumption on biocathodes.

Fresh YTF medium is filled in both chambers of the electrochemical H-cells. To initiate biofilm formation, 10% (v/v) of the pre-grown culture was transferred in the cathode chamber of the H-cell. The culture was continuously sparged with CO₂:N₂ = 20%:80% gas (5 sccm flow rate) and heated to 37 °C. Optical density at 600 nm (OD₆₀₀) was measured periodically every ~24 h. (Fig. S4d-f). Also, 1 ml aliquots were collected to measure concentrations of consumed fructose and produced acetate and ethanol. Afterwards, at each time point 2/3 of the electrolyte was replaced with fresh YTF medium. The OD₆₀₀ and pH value after medium refreshment were maintained at ~ 0.2 and ~ 6.1 (Fig. S4c), respectively. After each refreshment biocathodes were characterized electrochemically as described below. Medium refreshment and analytical experiments were repeated until culture (*i.e.* planktonic cells) reached the stationary phase (Fig. S4).

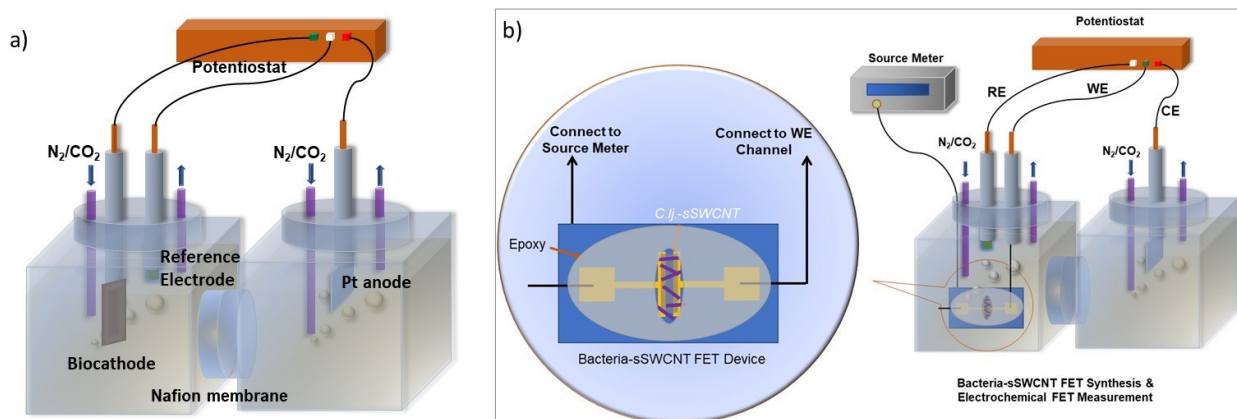


Figure S3. Scheme of the H-cell used in the electrochemistry set up. RE-reference electrode Ag/AgCl; CE-counter electrode Pt. a) Standard experimental set up with C-felt (+/- SWCNT) working electrode (WE), b) Set up for gating experiments with SWCNT films spanning source and drain electrode gaps.

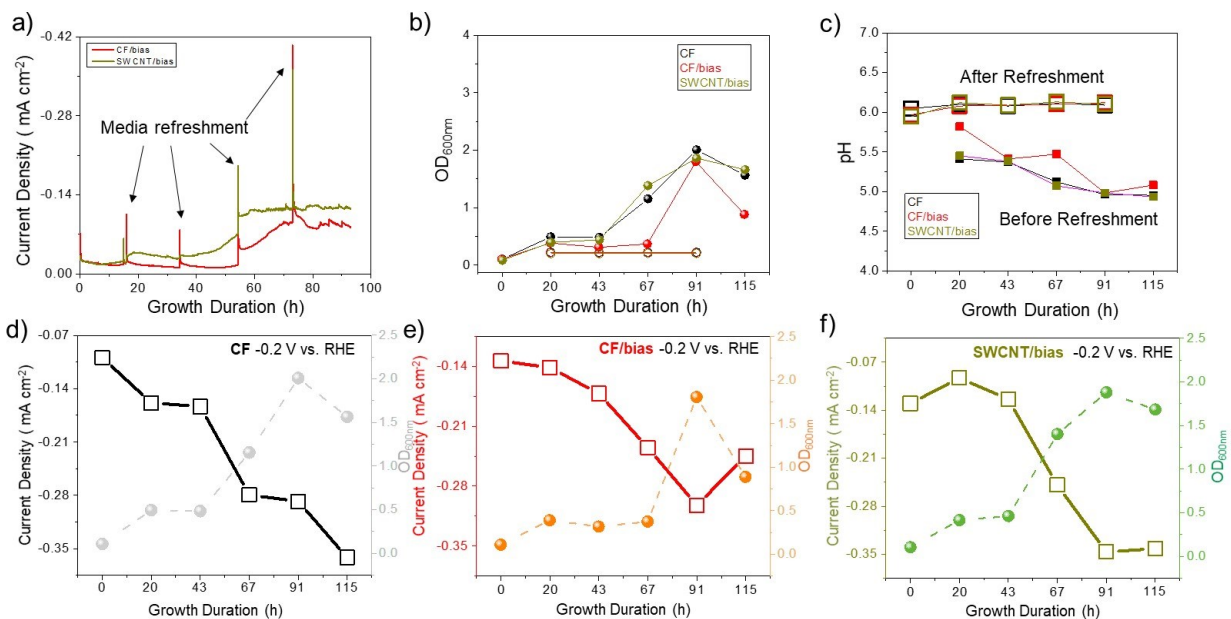


Figure S4. *Growth phase* a) Amperometric *i-t* curves at applied -0.7 vs Ag/AgCl for CF/bias and SWCNT/bias electrodes. The current spikes are related to the media refreshment. b) Comparison of growth of planktonic cell in the media for all 3 electrodes measured as changes in OD₆₀₀. c) Hollow square curve indicates the media pH change during the growth phase was kept around 6.1 after refreshing the YTF media every 20 h. Corresponding pH values before the media refreshment everyday are shown by the solid square curve. Changes in OD₆₀₀ in liquid cultures (i.e. from

planktonic cells) and changes in reduction current density taken at -0.2V vs RHE, scan rate 5 mVs⁻¹ for d) CF, e) CF/bias and f) SWCNT/bias electrodes.

Consumed fructose and produced acetate and ethanol were measured during the growth phase in the YTF media/electrolyte (Fig S5a). Calculated values for acetate and ethanol produced from fructose consumption are shown in Fig. S5b). It appears that after 115 h in the growth phase ~ 50% of C2 products were produced autotrophically from CO₂ reduction. It also appears that applied potential on the electrode has no effects on cells activities in solution, i.e. there is no electro-enhanced fermentation.

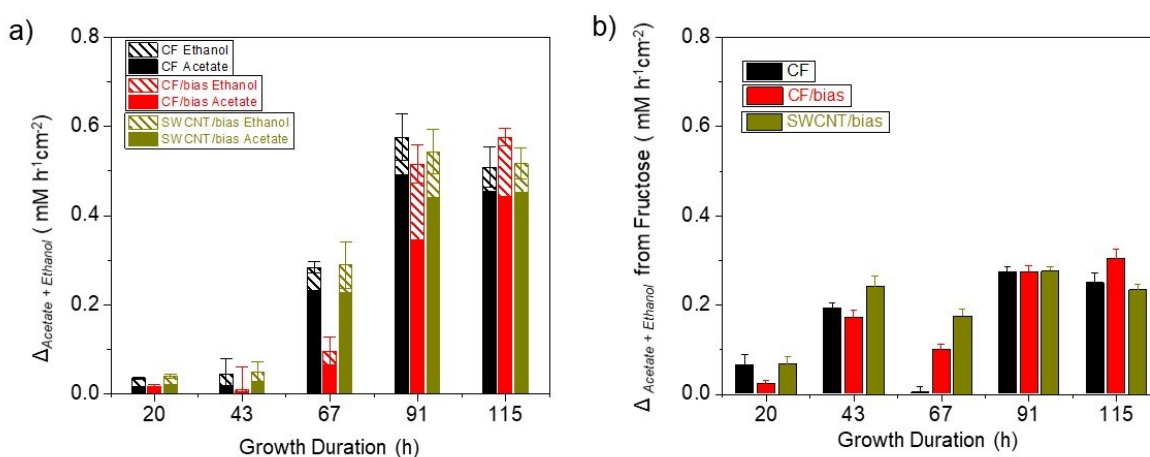


Figure S5. a) Produced C2 products (acetate and ethanol) were measured during the growth phase in the YTF media/electrolyte. b) Calculated production of acetate and ethanol based on fructose consumption data.

***C. ljungdahlii* biofilms on CF and CF/SWCNT electrodes in the electrochemical phase (EC Phase):**

After the *Growth Phase* biocathodes were taken out of YTF media and gently washed with phosphate-buffered saline (PBS) solution. Biocathodes were inserted in modified 1754 PETC media (ATCC) and experiments were run at constant reducing potential -0.05 V vs RHE (amperometric i-t measurements). Other conditions were identical to *Growth Phase*. Periodically (every ~24 hours) 1 ml aliquots were taken to measure acetate and ethanol in solution. LSV measurements were also conducted to monitor biofilm electroactivities. During the experiment, the applied potential was interrupted temporarily to collect aliquots and conduct LSV measurements, which caused the spikes in the i-t curves. At each test point, the pH of the

electrolyte was monitored. In the manuscript we report voltage versus reversible hydrogen electrode (RHE), which were calculated based on following equation:

$$E \text{ (vs. RHE)} = E \text{ (vs. Ag/AgCl)} + 0.209 + 0.059 \times \text{pH}$$

The overpotential ΔE observed in LSVs during EC phase is defined as the voltage difference between the electrochemical working potential and the thermodynamic potential for CO₂ reduction (at pH=7.4) into acetic acid:

$$\Delta E = E \text{ (vs. RHE)} - 0.17$$

The modified PETC medium:

NH₄Cl 1.0 gL⁻¹

KCl 0.1 gL⁻¹

MgSO₄·7H₂O 0.2 gL⁻¹

NaCl 0.8 gL⁻¹

KH₂PO₄ 0.1 gL⁻¹

CaCl₂·2H₂O 20.0 gL⁻¹

NaHCO₃ 2.0 gL⁻¹

Trace Elements (see below) 10.0 mL⁻¹

Wolfe's Vitamin Solution (see below) 10.0 mL⁻¹

Trace Elements:

Nitrilotriacetic acid 2.0 gL⁻¹

MnSO₄·H₂O 1.0 gL⁻¹

Fe(SO₄)₂(NH₄)₂·6H₂O 0.8 gL⁻¹

CoCl₂·6H₂O 0.2 gL⁻¹

ZnSO₄·7H₂O 0.2 mgL⁻¹

CuCl₂·2H₂O 20.0 mgL⁻¹

NiCl₂·6H₂O 20.0mgL⁻¹

Na₂MoO₄·2H₂O 20.0mgL⁻¹

Na₂SeO₄ 20.0mgL⁻¹

Na₂WO₄ 20.0mgL⁻¹

Wolfe's Vitamin Solution:

Biotin 2.0 mgL⁻¹

Folic acid 2.0 mgL⁻¹

Pyridoxine hydrochloride 10.0 mgL⁻¹

Thiamine . HCl 5.0 mgL⁻¹

Riboflavin 5.0 mgL⁻¹

Nicotinic acid 5.0 mgL⁻¹

Calcium D-(+)-pantothenate 5.0 mgL⁻¹

Vitamin B12 0.1 mgL⁻¹

p-Aminobenzoic acid 5.0 mgL⁻¹

Thioctic acid 5.0 mgL⁻¹

Chemical analysis

During Growth and EC Phase, aliquots of the electrolyte were collected periodically to measure consumed fructose (*Growth Phase*) and produced acetate and ethanol (*Growth and EC Phase*) by high-performance liquid chromatography (HPLC, Agilent Technologies). H₂ produced electrochemically, was measured in the headspace by gas chromatography (7890A GC system, Agilent Technologies).

Electrochemical characterization of biocathodes

Electrochemical measurements were conducted with single- and multi-channel potentiostats (CH Instruments) to monitor biofilm growth and electroactivities in the growth phase (Fig 4a). Linear sweep voltammetry (LSV), electrochemical impedance spectroscopy (EIS) were conducted before and after medium refreshment to check the biofilm formation on the cathode. LSV was scanned from 0 to -0.9 V (vs. Ag/AgCl) with the scan rate of 5 mVs⁻¹. Electrochemical impedance spectroscopy (EIS) under various potentials (-0.4 V, -0.8V) was used to characterize the charge transfer resistance between electrode and electrolyte. The amplitude was 10 mV, the frequency range is 0.01 Hz-100K Hz. The impedance data were analyzed with software CHI600e (CH Instruments, Inc.).

Biofilm characterization by electrochemical impedance spectroscopy (EIS)

Electrochemical impedance spectroscopy (EIS) can be applied as a non-intrusive method to monitor biofilm formation and growth. The measurement was taken after each media refreshment, where the constant electrolyte condition (OD_{600nm} , pH) was maintained (Fig. S4c). Bacteria attachment and biofilm formation on electrode surfaces displaces the electrolyte layer and changes the physicochemical nature of cathode-electrolyte interface. Biofilm formation typically includes a series of steps. Initially, a bacterium attaches on the electrode surface reversibly. Irreversible attachment of a single bacterium is followed by the production of an extracellular matrix and fibrous structures, which increases stability and facilitates binding of other bacteria to form colonies. Thereafter, colonies transition to mature biofilms.

A simple equivalent circuit model (Fig. S6a, inset) was designed for fitting the EIS parameters: double-layer capacitance (C_{dl}), solution (R_s) and charge transfer resistance (R_{ct}). The constant phase element (CPE) was introduced to represent the C_{dl} of inhomogeneous electrode/electrolyte interface. The value of C_{dl} is defined by the following equation:³

$$C_{dl} = \varepsilon \varepsilon_0 A / d \quad (1)$$

where ε is the dielectric constant of the electrolyte, ε_0 (8.854×10^{-12} F/m) is the permittivity of free space, d is the thickness of the double-layer, and A is the electrode area. The impedance data were analyzed based on an equivalent circuit model, utilizing software (CH Instruments, Inc.). CPE_t and CPE_0 are the constant phase element (CPE) representing double-layer capacitance in the modeling procedure at the specific and initial time measurements, respectively. The percent change in double-layer capacitance (ΔC_{dl}) was determined based on following equation:

$$\Delta C_{dl} = \frac{CPE_t - CPE_0}{CPE_0} \times 100\%$$

Changes in double-layer capacitance (ΔC_{dl}) are shown in Fig. S9a for all 3 electrodes. Biofilm adhesion during the rapid phase (after ~ 20 h – 90 h) of cells growth decreases surface double-layer charging, leading to decrease in ΔC_{dl} . Interestingly the ΔC_{dl} changes trend from positive to negative after 20 hours, suggesting different steps in biofilm formation, which is similar to previous study,⁴ possibly corresponding to reversible versus irreversible cell attachment. A plateau appears after 67 h, suggesting biofilm maturation. Similar to Nyquist plots, increases in ΔC_{dl} in the first phase are more significant for electrodes prepared under applied bias, while in the second

phase there is no significant difference for different electrodes. This might imply that applied bias has significant effect in the early phases of biofilm growth (i.e. on bacteria attachment), but not on colony maturation.

Nyquist plots for four different biocathodes (CF, CF/bias, SWCNT/bias) are presented in Fig. S6b-d, where the diameter of the semicircle at the high-frequency range represents R_{ct} . Decreases in R_{ct} values imply that electrons can escape electrode surface more easily and are more available for the reduction reactions in the presence of biofilms. Overall decrease in R_{ct} values for all four electrodes with biofilm growth are also shown in Fig. S6b-d. Based on the LSV data (Fig. 2b) and thermodynamic redox potentials for proton and CO_2 reduction (0 and 0.17 V vs RHE, respectively), we assume reducing currents at -0.2V and only capacitive currents at +0.2V, suggesting *faradic* and *non-faradic* conditions respectively. Decreases in R_{ct} values at -0.2V vs RHE with biofilm growth were highest for SWCNT/bias and CF/bias biocathodes, suggesting higher electrocatalytic activities for biofilm growth under applied bias and on SWCNT films. Biofilms grown under applied bias could express biomolecules that facilitate EET and CO_2 reduction, that are active under more negative potentials (i.e. faradic conditions). Overall trends for changes in R_{ct} values at 0.2V vs RHE were more complex, with lower R_{ct} for SWCNT functionalized electrodes.

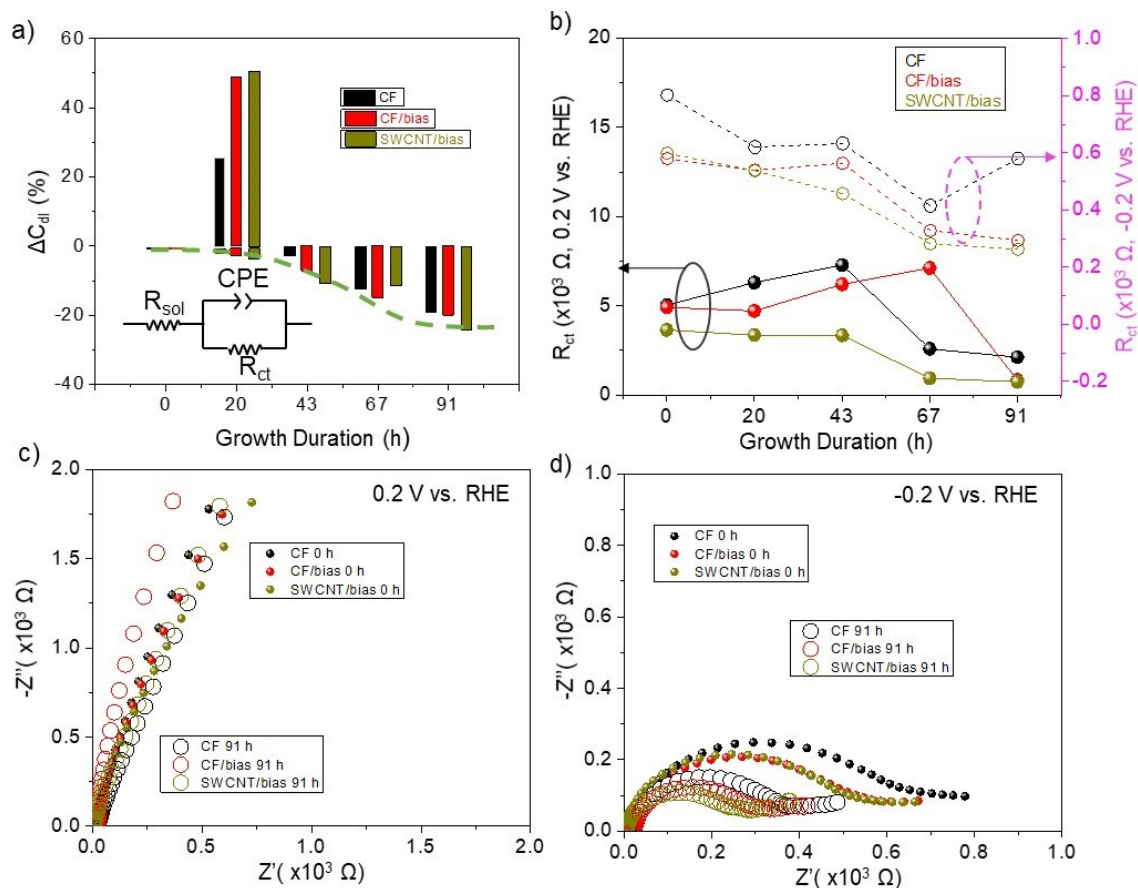


Figure S6. Electrochemical impedance spectroscopy (EIS) measurements in Growth phase **a)** percent change in double-layer capacitance (ΔC_{dl}) during biofilm growth. **b)** changes in charge transfer resistance (R_{ct}) for all four bioelectrodes under none-faradic conditions (0.2 V) and faradic conditions (-0.2 V) and **c)** Nyquist plots collected at 0.2 V and **d)** -0.2 V.

Electron microscopy characterization of biocathodes (SEM, TEM)

The biofilms were fixed in 2.5% glutaraldehyde in phosphate buffer under 4 °C for 2 h. The samples then underwent a MilliQ water postfix wash and dehydration (~ 24 h in a vacuum desiccator). Scanning Electron Microscopy (FEI Quanta SEM 600) was applied to characterize the surface morphology as well as the cell loading density. Samples were imaged at 3 kV acceleration, 7–10 mm working distance. Transmission electron microscopy (FEI F20) was applied to characterize some samples at the individual bacterium level. For TEM the sample was collected by scraping biocathode surface and transferring debris to a regular TEM copper grid (TED PELLA, INC. Part No. 01894-F).

Field-effect transistors (FET) measurements

The semiconductor single-walled carbon nanotube (SWCNT) field-effect transistor (FET) device was fabricated by using an ultrasonic spray coater to spray as-prepared plasma torch-sWCNT inks to pre-patterned 200 nm SiO₂/Si substrate. SiO₂/Si substrate is fabricated by using standard microfabrication process in the cleanroom. The electrode is prepared by depositing 5nm Ti/20nm Au through thermal evaporation. There are three channels on each device chip. The dimension of channel tested in this study is 10 μm (width) × 1000 μm (length).

The biofilms were grown on s-SWCNT FET as follows: the source, drain and gate contacts were connected with Cu wires. Next, FET device was sealed with epoxy leaving only the s-SWCNT deposited channel area exposed. Biofilms are prepared under the same conditions as described earlier for the growth phase, with source or drain pad connected to the potentiostat working electrode (WE) channel (Fig. S3b). The device was immersed in the catholyte contained *C.lj.* culture. Once biofilms were formed, the FET device was gently washed with PBS buffer. The exposed bacteria-modified s-SWCNT channel area was filled with modified PETC medium (as in the EC phase) for the charge transfer test. FET measurements were conducted with a probe station platform, two Keithley 2400 source meters, and a laptop with LabVIEW control programs, and the whole system is built and studied in the nitrogen-filled glovebox. For FET measurements the gate voltage (V_G) is swept in the range -10V to 10V, with sweep rate 4.41V/s. Thereafter, the device was used as working electrode for EC phase process (see above method details), where the different constant gate voltages (-3V, 0V, -3V) were applied during the whole process. LSV were recorded and samples were collected every day to analyze the production of acetate acid.

Isotope Experiments

¹³C-labeled CO₂ (99%, Cambridge Isotope Laboratories) was added (~ 9.5%) to the purging gas during the growth and EC phase to monitor the CO₂ reduction and incorporation into products. ¹³C-labeled/¹²C-labeled acetate ratio was measured by gas chromatography-mass spectrometry (GC-MS) and ¹³CNMR techniques before and after the ¹³CO₂ sparging period. ¹³C-labeled ethanol (¹³CH₃¹³CH₂OH, 99%, Sigma-Aldrich) was added in concentrations 0.5 mM during EC phase. ¹³C-labeled/¹²C-labeled acetate was determined by NMR (Bruker pulse program noesypr1d).

20% D₂O was added to cathode electrolyte during the EC phase, with biocathodes kept at two different potentials (-0.6 or -0.8 vs. Ag/AgCl). D₂O concentrations above 20% were not used due to D₂O toxicity to *C. ljungdahlii* cells. The gas chromatography-mass spectrometry (GC-MS) was utilized to analyze the labeled H in the products.

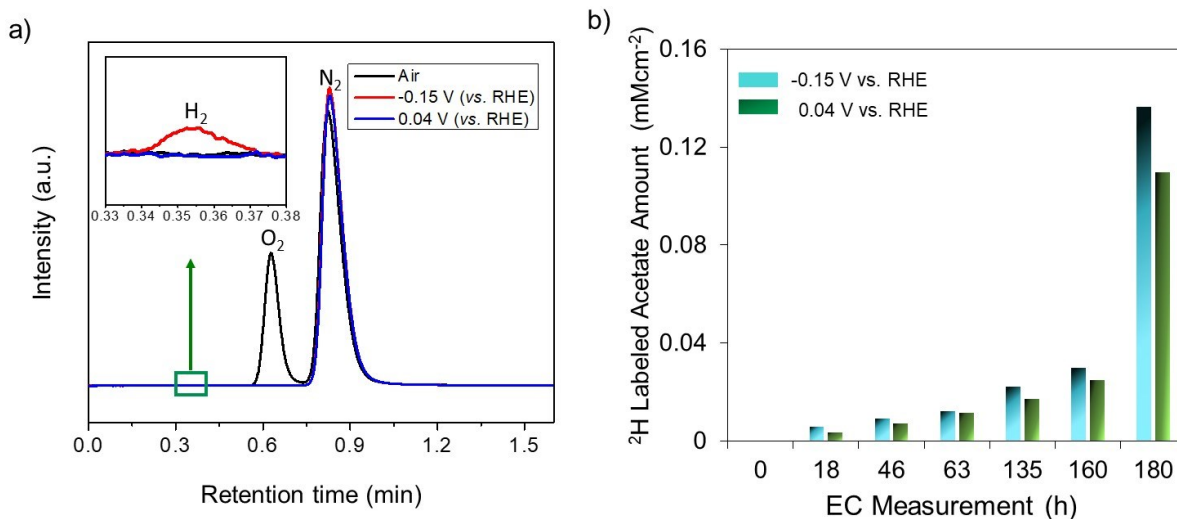


Figure 7. a) Gas chromatography analysis of the head space from the cathodic department. Hydrogen evolution did not occur at 0.04 V (vs. RHE) but evolved electrochemically at more negative potential (-0.15 V vs. RHE). **b)** Increases in concentration of *total* ²H labeled acetate produced in the EC phase for SWCNT/bias electrode. **Note:** more *total acetate* (labeled and unlabeled) is produced at more negative potential, while the *fraction of labeled acetate* (concentration of labeled acetate divided by total acetate) is higher at more positive potentials (Figure 4b).

Optimizing SWCNT ink concentrations

To optimize MES activity, we prepared a series of samples in which CF was treated with varying amounts of SWCNTs. Relative SWCNT loading was controlled by the concentration of the dispersion used to functionalize the CF electrode and was confirmed by Raman spectroscopy (see Fig. S1c). Acetate production was measured periodically for CF/bias biocathode and SWCNT/bias biocathodes kept at -0.05V (vs. RHE) for more than 5 days. Acetate production rates from CO₂ only ($\delta_{Acetate}$) at -0.05V (vs. RHE) for CF/bias biocathode and SWCNT/bias biocathodes were calculated from ¹³CO₂ labeling experiments. It appears that significant increases in SWCNT coverages (Fig S1c) does not result in a proportionate increase in ($\delta_{Acetate}$).

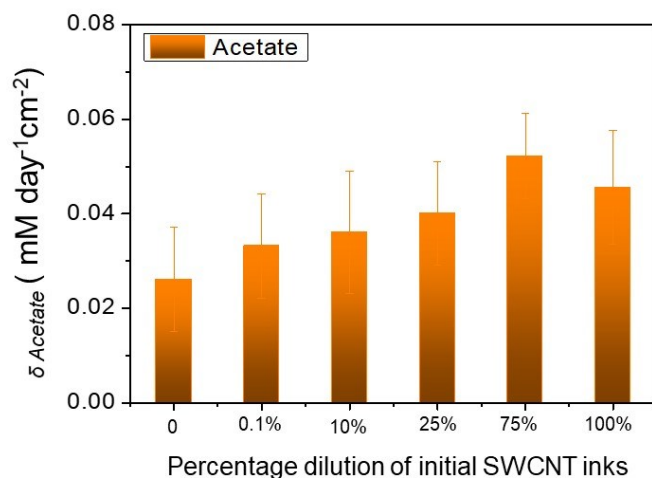


Figure S8. Acetate production rate measured based on ¹³CO₂ labeling experiments in the EC phase for CF/bias control and SWCNT/bias biocathode with various SWCNT coverages. There is an obvious trend with the highest acetate production with electrodes prepared with 75% SWCNT ink, which was 2-fold higher than acetate production activities of unfunctionalized CF.

Ethanol measured in EC phase

From the beginning of EC phase we saw significant concentrations of ethanol in the solution.

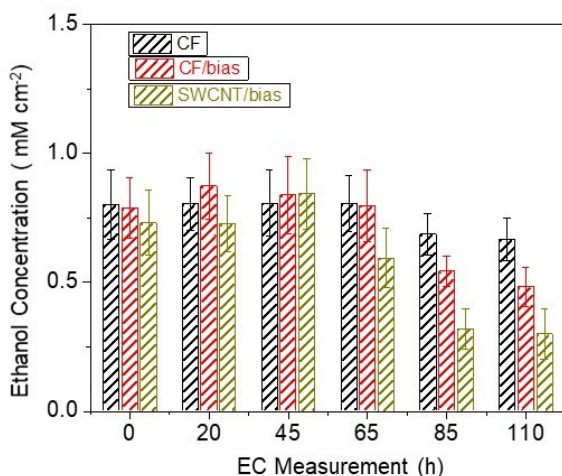


Figure S9. Time dependent ethanol concentration measured in solutions for 3 different bioelectrodes. All the data are from 3 bio-replicates. Produced acetate and conditions are described in the main text (Figure 4b.)

CO₂ isotope experiments

. We have conducted ¹³CO₂ isotope experiments in order to separate organotrophic from autotrophic (CO₂ reduction) activities. That was also necessary to calculate concentrations of acetate from CO₂ reduction and Faradic efficiencies for different bioelectrodes. For ¹³CO₂ labeling experiment the headspace gas contained only fraction of ¹³C-labeled gas (Fig. S10 a and b). As show in Fig. S10b and Table S1, the significantly smaller ¹³C labeled acetate ratio from all bioelectrodes compared to total ¹³CO₂ percentage (α in Fig. S10b) in the fixed period suggests that the CO₂ mass transport in the electrolyte is slow. Also, there is no obvious production of labeled acetate and ethanol under “no electrochemistry (EC) applied” condition (Fig. S10c).

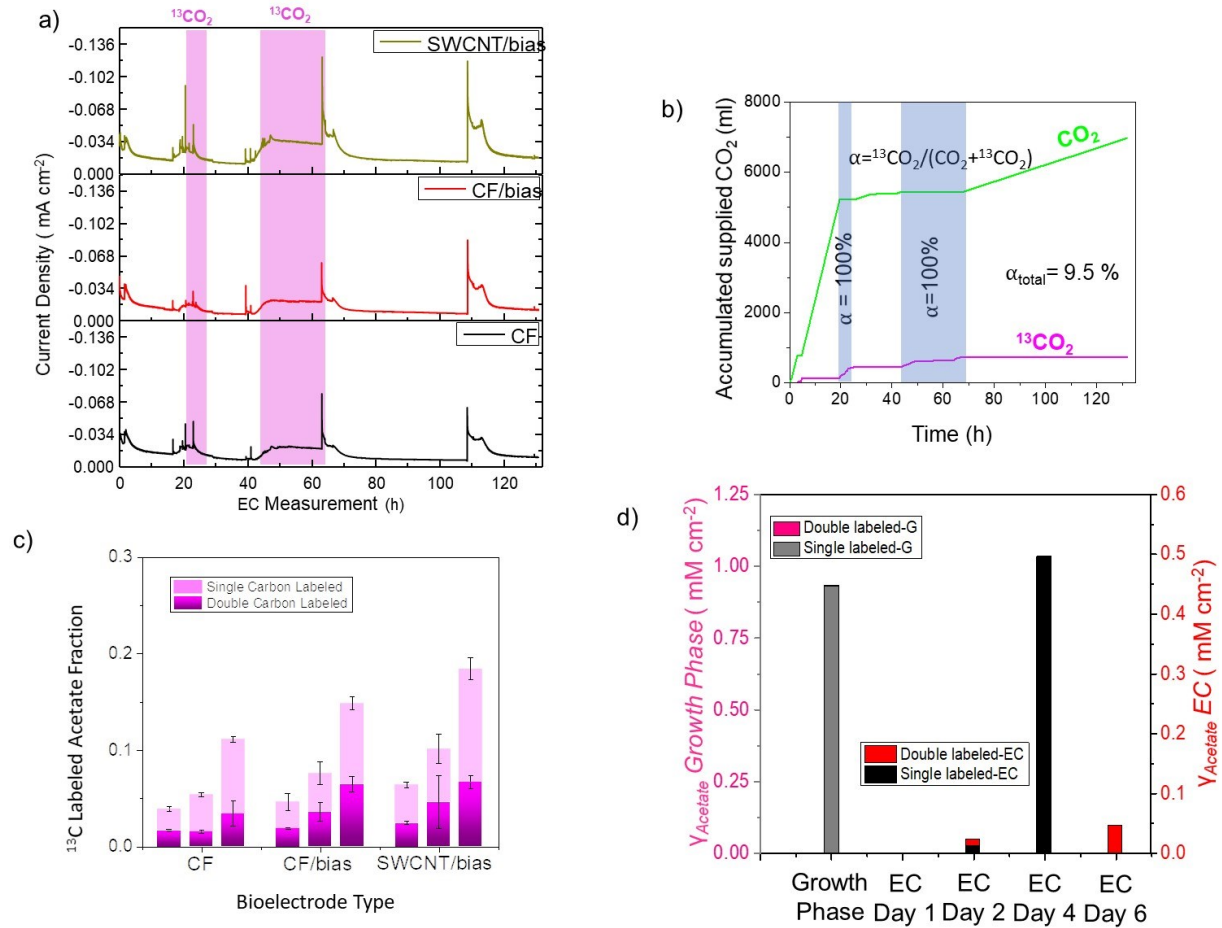


Figure S10. a) i-t curve of 4 bioelectrode in the EC phase. Pink area indicating the ¹³CO₂ supply period. b) The accumulated supply volume of CO₂ and ¹³CO₂ in the whole EC phase. c) ¹³C labeled acetate as a fraction of total acetate produced during EC phase. Data show acetate fraction after 135 h in the EC phase. Concentrations of labeled acetate were measured either by GC-MS as described in Supplemental. d) Production of labeled acetate detected in the 4th day of EC phase when ¹³CO₂ was supplied only in the growth phase.

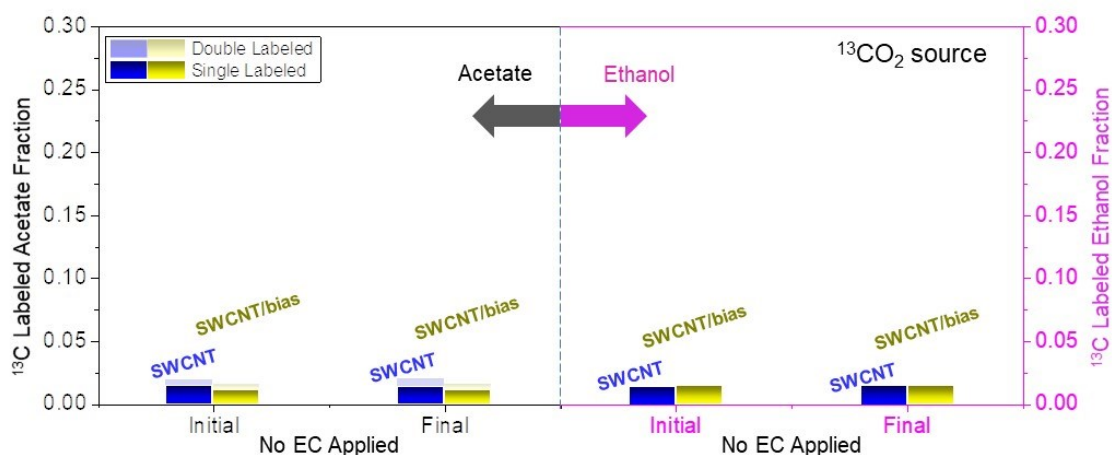


Figure S11. $^{13}\text{CO}_2$ labeling experiments showing there is no obvious production of labeled acetate and ethanol under “no electrochemistry (EC) applied” condition.

Table S1. Summary for $^{13}\text{CH}_2^{13}\text{CH}_3\text{OH}$ and $^{13}\text{CO}_2$ labeling experiments. Numbers represent the fraction of total acetate product.

	Electrode	Time	$^{12}\text{CH}_3^{12}\text{C O}_2^-$	$^{12}\text{CH}_3^{13}\text{CO}_2^-$	$^{13}\text{CH}_3^{12}\text{CO}_2^-$	$^{13}\text{CH}_3^{13}\text{CO}_2^-$
$^{12}\text{CO}_2:^{13}\text{CO}_2$ ~ 9:1	CF	20 h	0.76196	0.02205	0.01754	0.01542
		26 h	0.94632	0.03826	0.03428	0.03599
		110 h	0.88889	0.07683	0.06469	0.06680
	CF/bias	20 h	0.95335	0.02718	0.01947	0.01542
		26 h	0.92411	0.03990	0.03599	0.03599
		110 h	0.85196	0.08335	0.06469	0.06680
	SWCNT/bias	20 h	0.93549	0.03947	0.02504	0.04642
		26 h	0.89879	0.05479	0.04642	0.04642
		110 h	0.81605	0.11715	0.06680	0.06680

Faradaic efficiency calculations

With the $^{13}\text{CO}_2$ experiment data, Faradaic efficiency, ($FE_{Acetate}$) was calculated based on the following equation:

$$FE_{Acetate} = \frac{8 \times (\Delta n_{^{13}\text{C} - \text{double labeled Acetate}} + \Delta n_{^{13}\text{C} - \text{single labeled Acetate}}) \times F}{\int I dt}$$

Where $\Delta n_{^{13}\text{C-double labeled Acetate}}$ and $\Delta n_{^{13}\text{C-single labeled Acetate}}$ are the change of ^{13}C -double labeled and ^{13}C -single labeled acetate amount difference between two sampling points, respectively. F is the Faraday constant, and $\int I dt$ is the amount of charge that has been passed through the working electrode during the sampling period.

Table S2. Summary of the acetate Faradaic efficiency for 3 bioelectrodes in this study.

Bioelectrode	$FE_{Acetate}$ (%)
CF	52
CF/bias	71
SWCNT/bias	91

^{13}C -SWCNT isotope experiments

We also used ^{13}C -labeled SWCNTs for CF functionalization and measured if the *C.lj.* could utilize solid carbon as carbon substrate for acetate production. Both acetate and ethanol showed the very low ^{13}C labeled fraction around ~1% for 7 days electrochemical process, which is usually the natural background abundance.

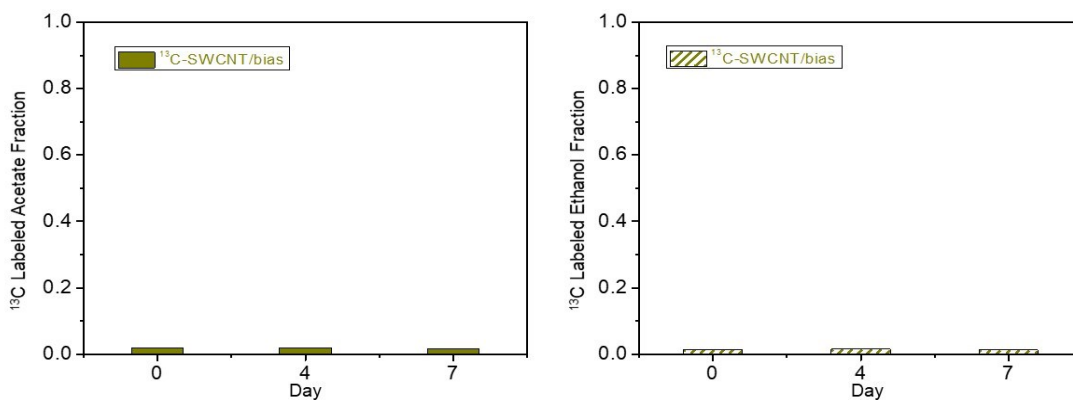


Figure S12. ^{13}C -SWCNT labeling experiments showing there is no obvious production of labeled acetate and ethanol during the *C. lj* biofilm growth and EC phase.

Estimation of bacteria coverages

Based on a visual inspection of SEM images with different magnification, it appeared that there were no differences in biofilm coverages for 3 electrodes (CF, CF/bias and SWCNT/bias).

The cell coverage was estimated using a previously reported method^{5,6}. Briefly, SEM images (270x) for all 3 electrodes were overlapped with a grid. The cells coverages for each grid section (80x80 μm) were counted and statistical averages were calculated. For each electrode 3 SEM images were analyzed.

Table S3. Summary of the acetate molecule production rate of all bioelectrodes in this study. Data are collected based on ^{13}C -acetate production electrochemistry phase.

Bioelectrode	δ_{Acetate} (mM day ⁻¹ cm ⁻²)	σ (cells μm^{-2})	γ (cell ⁻¹ s ⁻¹)
CF	0.0166 \pm 0.014	0.1736 \pm 0.08	(4.33 \pm 0.10) $\times 10^5$
CF/bias	0.0261 \pm 0.011	0.1964 \pm 0.08	(6.79 \pm 0.08) $\times 10^5$
SWCNT-0.1%/bias	0.0332 \pm 0.011	0.1956 \pm 0.06	(7.69 \pm 0.14) $\times 10^5$
SWCNT-10%/bias-2	0.0361 \pm 0.013	0.2012 \pm 0.05	(8.13 \pm 0.10) $\times 10^5$
SWCNT-25%/bias-3	0.0401 \pm 0.011	0.1988 \pm 0.04	(9.14 \pm 0.07) $\times 10^5$
SWCNT-75%/bias-4	0.0522 \pm 0.009	0.2076 \pm 0.07	(1.14 \pm 0.13) $\times 10^6$
SWCNT-100%/bias-5	0.0456 \pm 0.012	0.1988 \pm 0.04	(1.04 \pm 0.14) $\times 10^5$

References

- 1 Norton-Baker, B. *et al.* Polymer-Free Carbon Nanotube Thermoelectrics with Improved Charge Carrier Transport and Power Factor. *ACS Energy Letters* **1**, 1212-1220, doi:10.1021/acscenergylett.6b00417 (2016).
- 2 Pochorovski, I. *et al.* H-bonded supramolecular polymer for the selective dispersion and subsequent release of large-diameter semiconducting single-walled carbon nanotubes. *J Am Chem Soc* **137**, 4328-4331, doi:10.1021/jacs.5b01704 (2015).
- 3 Brug, G. J., van den Eeden, A. L. G., Sluyters-Rehbach, M. & Sluyters, J. H. The analysis of electrode impedances complicated by the presence of a constant phase element. *Journal of Electroanalytical Chemistry and Interfacial Electrochemistry* **176**, 275-295, doi:10.1016/s0022-0728(84)80324-1 (1984).
- 4 Kim, T., Kang, J., Lee, J.-H. & Yoon, J. Influence of attached bacteria and biofilm on double-layer capacitance during biofilm monitoring by electrochemical impedance spectroscopy. *Water Research* **45**, 4615-4622, doi:10.1016/j.watres.2011.06.010 (2011).
- 5 Liu, C. *et al.* Nanowire–Bacteria Hybrids for Unassisted Solar Carbon Dioxide Fixation to Value-Added Chemicals. *Nano Letters* **15**, 3634-3639, doi:10.1021/acs.nanolett.5b01254 (2015).
- 6 Wang, F., Hwang, Y., Qian, P. Z. G. & Wang, X. A Statistics-Guided Approach to Precise Characterization of Nanowire Morphology. *ACS Nano* **4**, 855-862, doi:10.1021/nn901530e (2010).